3. Z. Bakonyi, D. Michaelis, U. Peschel, G. Onishchukov, and F. Lederer 'Dissipative Solitons and their Critical Slowing Down Near a Supercritical Bifurcation', J. Opt. Soc. Am. B (in press).
4. G.P. Agrawal "Fast-Fourier-transform based beam propagation model for stripe-geometry semiconductor lasers" J. Appl. Phys. 56, 3100–3108 (1984).

CTuT5 **6:00 pm**

Two-dimensional Polarization Switching of Lithium Niobate

L.-H. Peng, S.-M. Tsan, Y.-C. Zhang, Y.-C. Shih, and C.-C. Hsu, Institute of Electro-Optical Engineering, National Taiwan University, Taipei, 106 Taiwan, R.O.C., Email: peng@cc.ee.ntu.edu.tw

The use of quasi-phase-matching (QPM) technique to compensate the phase velocity difference in interacting optical waves has greatly revived the field of nonlinear optics. A plethora of research activity has benefited from the availability of periodically poled lithium niobate (PPLN) and lithium tantalate (PPLT). These structures are characterized by a periodical sign reversal in the second-order nonlinear susceptibility $\chi^{(2)}$ every coherent length, $l_c = \lambda_\omega/4(n_{2\omega} - n_\omega)$, to compensate the destructive interference caused by the material's dispersion in the refractive index, *n*. Great challenge, however, remains in manipulating the coercive and fringing field to achieve a high fidelity of pattern transfer in making fine QPM structure to raise up the conversion efficiency.[1]

To further enhance the wavelength capacity and increase the acceptance angle, a two-dimensional (2D) $\chi^{(2)}$ nonlinear photonic crystal has recently been proposed.[2] Such a new type of crystal preserves a space-independent linear dielectric constant but has a 2D distribution in the second-order nonlinear coefficient that is periodically reversed in sign. The Fourier transform of the 2D lattice structure and the domain shape, respectively, uniquely determines the QPM direction and the conversion efficiency. It is therefore desirable to develop a domain poling method to resolve a 2D nonlinear photonic crystal of arbitrary domain structure. However, it is found that the inverted domain tends to nucleate according to the crystal's point group symmetry, which in the case of $LiNbO_3$ belongs to 3*m*. A common practice is to align the patterned electrode such that the domain walls are formed parallel to the crystal *y*-axis and at $\pm 60°$ with respect to the *x*-axis. A genetic unit cell in the $LiNbO_3$ 2D $\chi^{(2)}$ nonlinear crystal therefore has a domain pattern of hexagon or triangle in shape and has a dimension on the order of 10 μm.[3]

In this work, we demonstrate a proof-of-concept mechanism that is not only capable of suppressing the fringing field effect but also generating a 2D $\chi^{(2)}$ $LiNbO_3$ domain pattern of arbitrary shape. This method takes advantage of the polarization-induced positive charge effect, i.e., $\nabla \cdot P_s = \rho$, at the shallow inverted domain boundary to constrain the lateral 180° domain motion in a subsequent pulsed field poling process. We thereby are able to achieve a 2D differential polarization switching on $LiNbO_3$ and obtain domain walls of arbitrary shape such as arc, ring, or rectangle for the first time. A periodically poled, $LiNbO_3$ $\chi^{(2)}$ photonic crystal with a cylindrical domain size as small as 3.3 μm has thus been achieved.

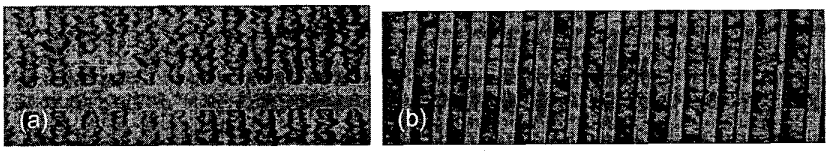

CTuT5 Fig. 1. Micrograph of the etched (a) +Z face of a heat-transformed Al_2O_3 electrode on $LiNbO_3$, and (b) the –Z face of an PPLN with a period of 5.1 μm.

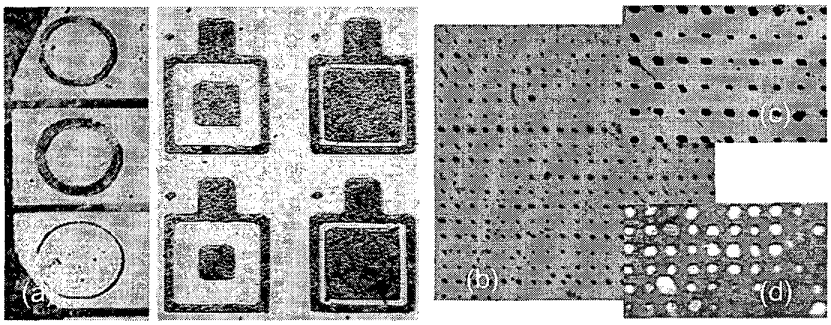

CTuT5 Fig. 2. Arbitrary 2D periodically poled structures on heat-treated $LiNbO_3$. The substrate thickness is 500 μm.

The micrograph of Fig. 1(a) reveals the hydrofluoric acid (HF) etched +Z face of a 10 μm-period Al-electrode after a heat-treatment at 1050°C. The etch pattern surrounding the Al_2O_3 electrodes indicates that a thin, surface domain inversion has taken place in the uncovered region.[4] We note that the heat-transformed Al_2O_3 electrode not only can preserve its underlying $LiNbO_3$ domain in its original polarization state, but also form a high-dielectric overlayer to facilitate the next-step of pulsed field poling.[5] One such example is shown in Fig. 1(b) for an etched –Z face of a 5.1 μm period PPLN poled at 22 kV/mm. Good control of the 5.1 μm periodicity over the 3 mm sample length and 500 μm-thick substrate has thus been realized.

In order to explore the heat-induced surface domain inversion effect on the lateral 180° domain motion, 2D poling is further examined on patterned electrodes that are *not* electrically interconnected. A 2D Al-thin film pattern of concentric ring-, or square-shape was first deposited on the +Z face of 500 μm-thick $LiNbO_3$ substrates and transformed to Al_2O_3 after heat treatment. Illustrated in Fig. 2(a) are the etch patterns on the –Z face of $LiNbO_3$ after the pulsed field poling. Inverted domain wall of arc, ring, or square in shape and as thin as 10 μm can thus be formed using this method. Note these arbitrary domain shapes, different from the crystal's trigonal symmetry, are created through a restraint over the 180° domain motion during the poling process. Our calculation shows that the restraining behavior is credited a localized charge distribution, resultant from the discontinuity of the spontaneous polarization P_s at the shallow, inverted domain boundary during the heat-treatment process. The positive charge distribution thereby can suppress the fringing field at the edge of the oxidized Al_2O_3 electrode, and thus inhibit the evasion of domain wall.

Last but not the least, the introduction of a surface domain inversion pattern on $LiNbO_3$ not only has proven as a method for suppressing the fringing field, but also promising for realizing a 2D periodically poled $\chi^{(2)}$ nonlinear crystal. Shown in Fig. 2(b) is the –Z face micrograph taken from a 15 μm × 20 μm $\chi^{(2)}$ rectangular lattice, and (c) the magnified picture of (b) revealing the details of the grid-poled domain structure. We note the lateral motion of the grid-like 180° poled domain stopped at the 15 μm × 20 μm rectangular boundary, which allows the $LiNbO_3$ conform to a 2D nonlinear crystal. In comparison, the magnified picture of Fig. 2 (d), taken from the –Z face of a 6.6 μm × 6.6 μm $\chi^{(2)}$ square lattice, presents a restrained motion of the cylindrical-like inverted domains that are not electrically interconnected. The lateral motion of the circularly-poled 180° inverted domain is inhibited by the surrounding positive charge at the shallow inverted domain boundary and form a domain size as small as 3.3 μm.

In summary, we report a two-step oxidation and switching process on Z-cut congruent grown $LiNbO_3$. By employing the polarization-induced positive charge effect at the inverted surface domain boundary, we enable a 2D differential switching mechanism that can lead to the formation of a 2D, $\chi^{(2)}$ nonlinear $LiNbO_3$ photonic crystal of arbitrary domain shape. This research was sponsored by the NSC Grant No. 90-2215-E-002-017.

1. R.G. Batchko, V.Y. Shur, M.M. Fejer, and R.L. Byer, "Backswitch poling in lithium niobate for high-fidelity domain patterning and efficient blue light generation," Appl. Phys. Lett. 75, 1673–1675 (1999).
2. V. Berger, "Nonlinear photonic crystals," Phys. Rev. Lett. **81**, 4136–4139 (1998).
3. N.G. Broderick, G.W. Ross, H.L. Offerhaus,

D.J. Richardson, and D.C. Hanna, "Hexagonally poled lithium niobate: a two-dimensional nonlinear photonic crystal," Phys. Rev. Lett. **84**, 4345–4347 (2000).
4. J. Webjörn, F. Laurell, and G. Arvidsson, "Blue light generated by frequency doubling of laser diode light in a lithium niobate channel waveguide," IEEE Photonic Technol. Lett. Vol. **1**, 316–319 (1989).
5. L.-H. Peng, Y.-C. Fang, and Y.-C. Lin, "Polarization switching of lithium niobate with giant internal field," Appl. Phys. Lett. **74**, 2070–2071 (1999).

CTuT6 **6:15 pm**

An Electro-optic Modulator Assisted by Nonlinear Coupling Dynamics

J.M. Fini and K.R. Tamura, Corlux Corporation, 47915 Westinghouse Rd., Fremont, CA 94539, Email: jfini@corlux.com

1. Introduction

At intensities where the Kerr effect plays a significant role, optical coupler show interesting nonlinear dynamics including bistable behavior. These dynamics are the basis for a family of all-optical switches.[1,2]

Here we propose using the bistability of a nonlinear coupler not for an all-optical switch, but to enhance the sensitivity of an electrically-controlled modulator. This is potentially of enormous benefit. Essentially all performance limitations of electro-optic modulators are related to the trade-offs in achieving a pi phase shift with a low drive voltage. By reducing the phase shift required for full switching, our scheme would loosen this fundamental constraint and allow higher bandwidth, lower power consumption, etc. We present simulations demonstrating the basic principle of the Kerr-assisted modulator, and calculate the moderate performance degradation due to optical power fluctuations.

2. Nonlinear coupler dynamics and enhanced modulation

A nonlinear directional coupler has two local waveguide modes which are coupled together at rate γ, each with a Kerr nonlinearity κ. The simplest model including these effects is a two-mode system:

$$idu/dz = -\gamma v - \kappa |u|^2 u$$

$$idv/dz = -\gamma u - \kappa |v|^2 v.$$

The Kerr effect tends to trap the optical intensity all on one side or all on the other of the coupler, by inducing an index difference between the waveguides. A properly designed coupler can show bistable behavior: light initially split evenly between the waveguides will couple completely into waveguide 1 or 2, depending on a small changes in initial relative phase. Thus small phase modulation can be converted into full amplitude modulation by using the bistability.

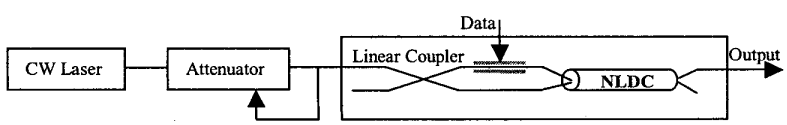

CTuT6 Fig. 1. Kerr-assisted modulator setup with input intensity monitor.

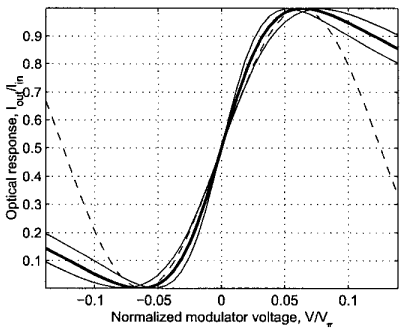

CTuT6 Fig. 2. Optical response of Kerr-assisted modulator shows an 8-times sensitivity enhancement.

The simplest proposed system (Figure 1) is almost identical to the standard external modulation setup: however, the output coupler is nonlinear, and the intensity and phase shift are biased at the bistable point described above.

We have simulated the modulator response using the simple model above, for normalized (κ = 1) values γ = .51, designed intensity $|u|^2 + |v|^2 = 1/2$, and length L = 5.92. An 8-times enhancement is obtained. The response is plotted in Figure 2. The three solid curves show the performance at the designed intensity (dark line) and with +/– 10% error in input intensity. The curve $\cos(\pi V/8V_\pi)$ is show for comparison (dashed). With these moderate variations in intensity, the modulator performance is still good, with a 19 dB extinction ratio.

The corresponding physical parameters will depend on the material and mode area. For example, 1 Watt input optical power may require coupler lengths of several centimeters for chalcogenide or hundreds of meters for conventional fiber.[3] Other candidates include GaAs [**Error! Reference source not found.**]. Pulsed implementations may allow higher intensities but have more severe dispersion issues.

Models including important group velocity dispersion and inter-modal dispersion have been examined.[2] In all-optical switching applications, nonlinear couplers must be designed to avoid performance degradation due to dispersive effects. The basic issues will be similar in our case. One can avoid degradation by operating in a quasi-cw regime where dispersion is small, or can utilize the inherent dispersion canceling properties of soliton-like pulses.[2,5]

References

1. S.M. Jensen, "The nonlinear coherent coupler," IEEE J. Quantum Electron., **18**, 158 (1982).
2. K.S. Chiang, "Propagation of short optical pulses in directional couplers with Kerr nonlinearity," J. Opt. Soc. Am. B, **14**, 1437 (1997).
3. G. Lenz, J. Zimmermann, *et. al.*, "Large Kerr effect in bulk Se-based chalcogenide glasses," Opt. Lett., **25**, 254 (2000).
4. N.S. Patel, K.L. Hall, and K.A. Rauschenbach, "Interferometric all-optical switches for ultrafast signal processing," Applied Optics, **37**, 2831 (1998).
5. C.R. Menyuk, "Stability of solitons in birefringent optical fibers. I. Equal propagation amplitudes," Opt. Lett., **12**, 614 (1987).

CTuU

4:45 pm–6:30 pm
Room: 104A

Super Continuum Generation and Solitons

Alexander Luis Gaeta, Cornell Univ., USA, Presider

CTuU1 **4:45 pm**

Route to Supercontinuum in Photonic Crystal Fibers

G. Genty, M. Lehtonen and H. Ludvigsen, Fiber-Optics Group, Metrology Research Institute, Helsinki University of Technology, P.O. Box 3000, FIN-02015 HUT, Finland, Email: goery.genty@hut.fi

M. Kaivola, Department of Engineering Physics and Mathematics, Helsinki University of Technology, P.O. Box 2200, FIN-02015 HUT, Finland

J.R. Jensen, Crystal Fibre A/S, Blokken 84, DK-3460 Birkerød, Denmark

Introduction

Recently, photonic crystal fibers (PCFs) have manifested themselves as efficient sources of supercontinuum (SC) radiation when pumped with short pulses of IR laser light.[1] Different nonlinear optical processes responsible for the generation of SC have been identified.[2,3] We have experimentally investigated the influence of the zero-dispersion wavelength on the SC generation and give here a qualitative analysis for the observed phenomena.

Experiments

To generate the supercontinuum, an 80-MHz pulse train from a tunable Ti:sapphire laser was coupled into a few meter-long PCF. The laser produces linearly polarized Gaussian pulses with a FWHM of 200 fs. The power of the input pulses was progressively increased in order to observe the evolution of the output spectrum towards supercontinuum. We investigated the formation of the continuum in two cases, i.e., when the pump pulse is located either in the anomalous or in the normal dispersion regime of the fiber.

Anomalous regime

To explore the SC generation when the pump pulse is located in the anomalous dispersion regime, we launched the pulse train into a highly birefringent PCF with core dimensions of 1.2 × 2.4 μm^2 and a zero-dispersion wavelength located at around 700 nm. Optical spectra of the output